

Investigation of Performance of Glass Fibre Impregnated with Bitumen Emulsion against Reflective Cracking

Ogundipe Olumide Moses*

Civil Engineering Department, Ekiti State University, Ado-Ekiti, Nigeria

Abstract

The study investigates the use of glass fibre impregnated with bitumen emulsion with 6mm aggregates compacted on it as a Stress Absorbing Membrane Interlayer (SAMI) to retard reflective cracking. The causes and mechanism of reflective cracking in an overlay over a cracked pavement were highlighted. Tests were carried out in a wheel tracking facility to induce modes I and II cracking. The effects of temperature, load level, composition of SAMI and overlay thickness on the performance of the SAMIs were evaluated. It was found that the two SAMIs investigated in this study were both able to retard reflective cracking. Better relative performance was observed with low overlay thickness and at high load level. Also, the study showed that temperature influenced the performance of the SAMIs and indicated that difference in the viscosity of the bitumen emulsion used in the SAMIs led to difference in performance. It was observed that the interface shear strain of the overlay-SAMI interface influenced the performance of the SAMI.

Keywords: Cracks; Overlay; Interlayer; Temperature; Load level

Introduction

The method commonly used to rehabilitate deteriorated pavements is by overlaying with a new surfacing material. Cleveland et al. [1] stated that for both flexible and composite pavements, a common technique used by many agencies for preventive maintenance and/or rehabilitation was simply to construct thin Hot Mix Asphalt (HMA) overlay, normally between 25 and 50 mm thick. Overlaying cracked pavements prevents water from infiltrating through the cracks into the pavement structure, thus preventing the deterioration of the pavement structure and increasing its structural capacity. Also, it reduces roughness, restores skid resistance, and improves the overall ride quality to the travelling public. However, it has been found that the cracks propagate through the overlay to its surface, a phenomenon called reflective cracking.

Reflective cracking can be defined simply as the propagation of existing cracks in an old pavement through the underside of the overlay to the surface. (Figure 1) shows a schematic of reflective cracking in HMA overlay on Portland Cement Concrete (PCC) slab or Asphalt Concrete (AC). Reflective cracking is often initiated at the bottom of the overlay material and grows until it appears at the surface. Also top-down cracking (cracks initiating at the surface and growing into the lower layers) occurs especially where there are large temperature variations in the pavement (thermal cracking).

A number of factors have been identified as the causes of reflective cracking. Palacios et al. [2] reported that cracks propagate to new overlays due to vertical movement of the underlying pavement layer which may be due to traffic loading, frost heave and consolidation of the sub grade soils and/or the horizontal movement of the pavement upper layers due to temperature changes. Quintus et al. [3] reported three causes of reflective cracking, the major being horizontal movements

from the expansion and contraction of the base pavement that is caused by temperature changes; the differential vertical deflections between the approach and departure slabs or across transverse cracks, which create shear stresses; and the curling of PCC slabs during colder temperature when the HMA overlay is stiff and brittle.

Abe et al. [4] stated that cracking was caused on the surface of the overlay at an early stage by the movement of the pavement and traffic load. Smith [5] also mentioned the differential vertical movement at a crack or slab joint in the old pavement which induces a vertical shear stress in the overlay, horizontal movement associated with temperature or moisture changes in the old pavement which induces tensile stress in the overlay or live load flexural stress in the overlay, which tends to concentrate directly over discontinuities. Based on the causes identified by researchers, there seems to be an agreement on the causes of reflective cracking. While it is common knowledge that factors such as sub grade conditions, pavement material quality, workmanship etc affect the performance of a pavement; the principal factors responsible for reflective cracking are the action of traffic loading on an overlay on a cracked pavement and thermal stresses developed as a result of daily/seasonal temperature variation. This study has concentrated on reflective cracking caused by the action of traffic loading.

It is important that the mechanisms of reflective cracking are well understood to be able to provide a solution to the problem. This is illustrated in Figures 2 and 3. Figure 2a depicts a situation where the moving wheel on the edge of the pavement above the crack produces maximum shear stresses, A and C respectively as shown in Figure 3, while in Figure 2b, the wheel directly on the overlay above the cracked pavement generates flexural stresses producing maximum bending stress, B as indicated in Figure 3. This illustration indicates two of the three modes of reflective cracking - Modes I and II. Molenaar [6]

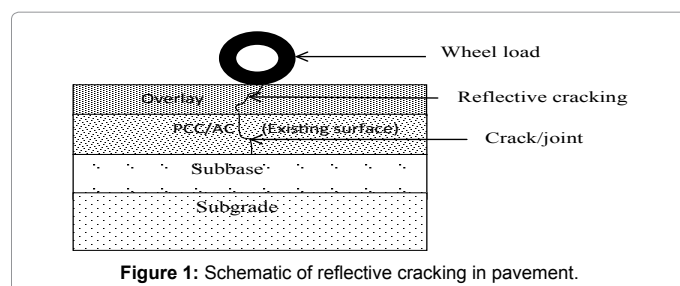


Figure 1: Schematic of reflective cracking in pavement.

*Corresponding author: Ogundipe Olumide Moses, Civil Engineering Department, Ekiti State University, Ado-Ekiti, Nigeria, Tel: +2348107825001; E mail: momide2002@yahoo.com

Received November 11, 2013; Accepted January 21, 2014; Published January 30, 2014

Citation: Moses OO (2014) Investigation of Performance of Glass Fibre Impregnated with Bitumen Emulsion against Reflective Cracking. J Civil Environ Eng 4: 137. doi:10.4172/2165-784X.1000137

Copyright: © 2014 Moses OO. This is an open-access article distributed under the terms of the Creative Commons Attribution License, which permits unrestricted use, distribution, and reproduction in any medium, provided the original author and source are credited.

established the three modes: mode I, mode II and mode III cracking. Mode I cracking occur due to tensile stresses caused by a drop in temperature or flexure under traffic loading. Mode II cracking is caused by the effects of shear stress induced by a loaded wheel crossing from one side of a transverse crack or joint to the other. Mode III, referred to as the tearing mode, is less common. This occurs in pavements when the wheel load travels along (parallel to) a crack. Figure 4 shows the three modes of cracking.

A number of measures have been adopted by engineers with the aim of retarding reflective cracking in overlays and results achieved have been mixed. These measures include: thick overlays, overlay mixture modification, overlay reinforcement, stress or strain absorbing interlayer's and reinforcing interlayer's. Al-Qadi et al. [7] stated that various interlayer materials namely: geosynthetics, geocomposites, steel reinforcement netting, and modified HMA, have been used as interlayer systems for the purpose of reducing reflective cracking, and that their effectiveness is still not well quantified due to lack of understanding of the reflective cracking mechanism and because imperfect evaluation approaches are used. No current pavement rehabilitation techniques have been shown to solve completely the problem of reflective cracking. This has been attributed to the number of variables that are involved in reflective cracking [8].

Sample type	Percent by composition of aggregate
10mm aggregate	37%
6 mm aggregate	26%
Dust	36%
Filler	1%
Binder type	10/20, 40/60 bitumen
Binder content	5.3% by mass of total mix
Target air void	5%

Table 1: Mix composition for 10 mm asphalt concrete.

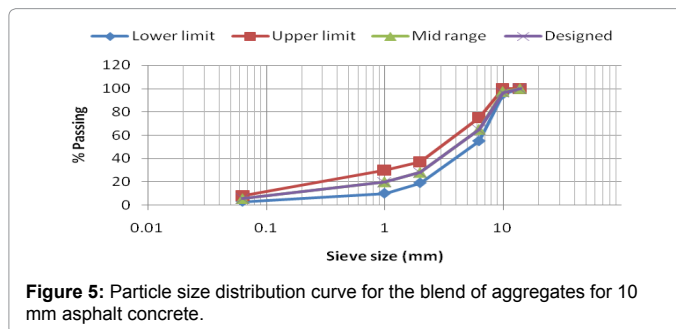


Figure 5: Particle size distribution curve for the blend of aggregates for 10 mm asphalt concrete.

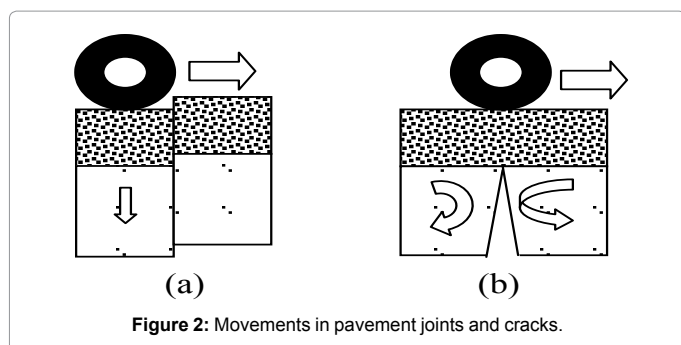


Figure 2: Movements in pavement joints and cracks.

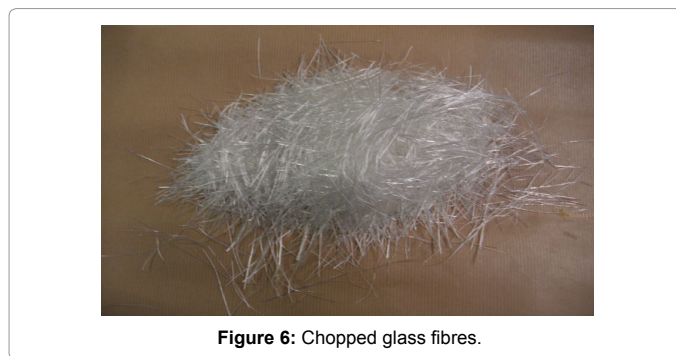


Figure 6: Chopped glass fibres.

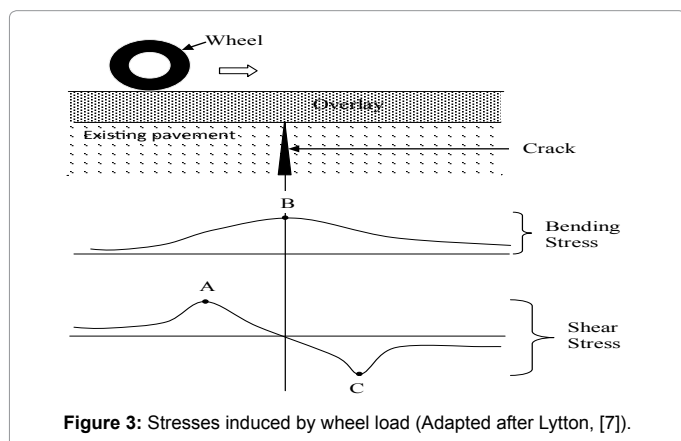


Figure 3: Stresses induced by wheel load (Adapted after Lytton, [7]).

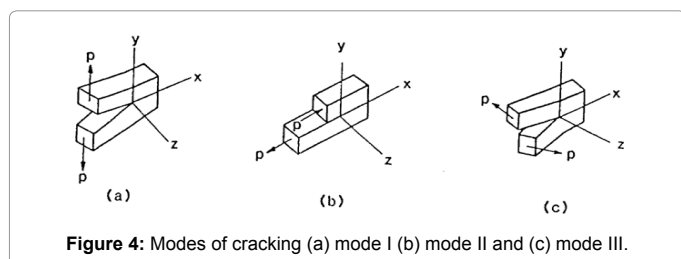


Figure 4: Modes of cracking (a) mode I (b) mode II and (c) mode III.

This research work aims to evaluate the contribution of a particular type of stress absorbing membrane interlayer (SAMI) designed to deform horizontally or vertically, therefore allowing the movement (vertical/horizontal) of the underlying pavement layers without causing large tensile stresses in the asphalt overlay. The effect of the SAMI on overlaid pavement performance in delaying reflective cracking and the influence of certain variables such as temperature overlay thickness, and load levels have all been studied.

Materials and Methods

Materials

The materials used in this study were as follows:

- 10 mm asphaltic concrete with 10/20 or 40/60 penetration grade bitumen. The mix composition is as shown in Table 1 and the particle size distribution curve for the blend of aggregates is shown in Figure 5.
- Proprietary SAMIs designated as SAMI 1 and SAMI 2. SAMI 1 is prepared by sandwiching chopped glass fibre shown in Figure 6 at 120 g/m² between layers of ordinary bitumen emulsion at 0.9 L/m² with 6 mm aggregates spread and compacted on top at a rate of 8 kg/m², while SAMI 2 varies in its use of polymer modified bitumen emulsion.
- A 10 mm thick rubber mat of 6.45MPa stiffness was used to simulate the pavement foundation.

Asphalt concrete (AC)	Stiffness (MPa)		
	Temperature		
	10°C	20°C	30°C
AC (40/60)	10000	3900	1100
AC (10/20)	15400	9600	5000

Table 2: Indirect tensile stiffness moduli.

Bitumen emulsion	Viscosity (Pa.s) @ 25°C	Viscosity (Pa.s) @ 30°C	Viscosity (Pa.s) @ 40°C
Ordinary bitumen emulsion	0.700	0.580	0.390
polymer modified bitumen emulsion	0.184	0.194	0.180

Table 3: Viscosity of bitumen emulsion.

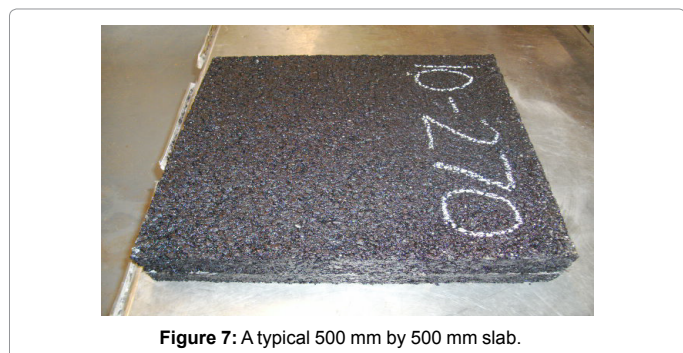


Figure 7: A typical 500 mm by 500 mm slab.

- The indirect tensile stiffness moduli (ITSM) of the mixtures were determined using the Nottingham asphalt tester (NAT) in accordance with British standard [9]. In the ITSM a load pulse is applied to the vertical diameter of a cylindrical specimen (100mm in diameter and 40mm thick) positioned centrally between the upper and the lower platens and the resultant peak transient deformation along the horizontal diameter is measured. The ITSM results for the 10mm asphalt concrete with 10/20 and 40/60 penetration grade bitumen at 10°C, 20°C and 30°C are shown in Table 2. The viscosity of the bitumen emulsion is shown in Table 3.

Methods

Sample preparation: The test specimens were made up of beams of length 404mm and width 50mm. The bottom (base) layer was a 30mm thick 10mm asphaltic concrete with 10/20 penetration grade bitumen, the middle layer (where present) was SAMI and the top layer (overlay) was a 10mm asphaltic concrete with 40/60 penetration grade bitumen.

The beams were obtained by manufacturing a slab of dimension 500 mm × 500 mm (Figure 7). For the base layer, the aggregates and binder were batched as shown in Table 1, heated at 185°C and compacted in a mould of dimension 500 mm × 500 mm × 205 mm with a roller compactor at a temperature of 180°C to a thickness of 30 mm. The SAMIs were prepared by sandwiching 60 mm glass fibre strands between layers of bitumen emulsion and 6 mm aggregates compacted over them. The aggregates for the top layer were batched as shown in Table 1, heated to 160°C and compacted to the required thickness at 150°C. All the mixtures were mixed in accordance with British standard [10] and compacted in accordance with British standard [11].

Ten beams of length 404 mm and width 50 mm were cut from each slab and a 10 mm wide notch was sawn at the centre of the beam through the 30 mm base layer to simulate the crack. Two aluminium brackets were glued to each side of the split base as LVDT measurement points. Typical beams with 10 mm notch in the base layer and aluminium brackets attached are shown in Figure 8.

Test procedure: The test was carried out by placing a 10mm thick rubber mat on the base of a steel mould on a reciprocating table. The beams were placed in a conditioning cabinet at test temperature for a minimum of five hours. The specimen sides were painted white to allow monitoring of crack growth during the test. The beams were placed in the steel mould on the wheel tracking facility and they were clamped at the top and sides to prevent them moving sideways. The Linear Variable Differential Transformers (LVDTs) were positioned on the aluminium brackets and connected to the data acquisition system. The specimens were trafficked and the numbers of wheel cycles for crack growth to the top of the overlay were recorded. The wheel tracker with a sample in place is shown in Figure 9. The test was carried out at 10°C, 20°C and 30°C. Two replicates were tested in each case. The test plan is shown in Table 4.

Test results and discussion: The results from the wheel tracking test were processed. Firstly, the number of wheel cycles for crack propagation to failure (crack appearing at the top of the overlay) was recorded for all specimens. The vertical displacements of the specimens during test were obtained from the LVDTs. The results presented are the averages of the replicates.

The specimen names and references used for the presentation of results are shown in Table 5. The results for the numbers of wheel cycles to failure at 10°C, 20°C and 30°C with a 2.4 kN (approximately 1.1 MPa) load applied are shown in Figures 10-12, respectively. Figure 13 shows the results at 30°C with a 1.35 kN (approximately 0.6 MPa) load applied. The figures show both SAMI 1 and SAMI 2 were able to increase the life of the overlay in most cases. Also, it can be seen from

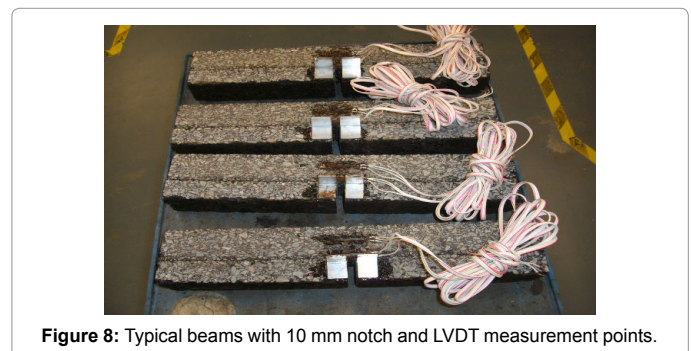


Figure 8: Typical beams with 10 mm notch and LVDT measurement points.

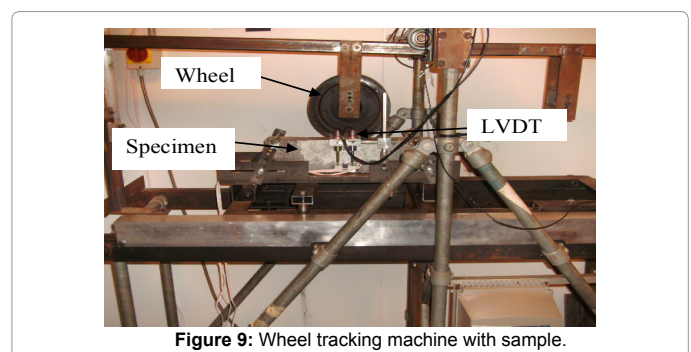


Figure 9: Wheel tracking machine with sample.

Load (kN)		2.4				1.35
Base thickness (mm)	Overlay thickness (mm)	Temperature (°C)				
		10	20	30	30	
30	40	√	√	√	√	
30	60	√	√	√	√	

Table 4: Test plan.

Specimen name	Specimen reference
40 mm Overlay (Control)	O40
SAMI 1 with 40 mm Overlay	SA1O40
SAMI 2 with 40 mm Overlay	SA2O40
60 mm Overlay (Control)	O60
SAMI 1 with 60 mm Overlay	SA1O60
SAMI 2 with 60 mm Overlay	SA2O60

Table 5: Specimen names and references.

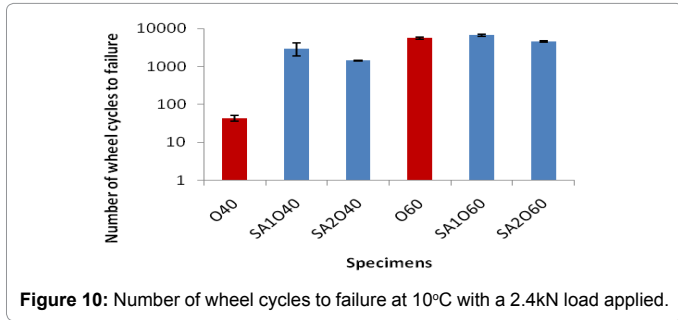


Figure 10: Number of wheel cycles to failure at 10°C with a 2.4kN load applied.

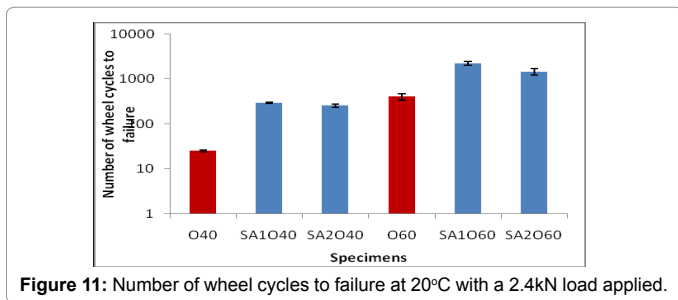


Figure 11: Number of wheel cycles to failure at 20°C with a 2.4kN load applied.

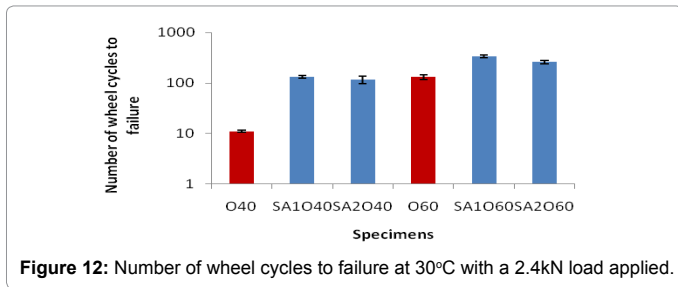


Figure 12: Number of wheel cycles to failure at 30°C with a 2.4kN load applied.

the figures that the specimens with SAMI 1 gave better performance than those with SAMI 2. This may be because the bitumen emulsion used in SAMI 2 was of insufficient viscosity, although the exact reason why this should give reduced performance is unclear.

Effect of load levels: Two load levels were used at 30°C: 2.4 kN (1.1 MPa) and 1.35 kN (0.6 MPa). The former is representative of tyre pressures on airfields and the latter representative of tyre pressures on highways. The numbers of wheel cycles to failure were normalized against the respective control specimens of equivalent thickness. The results as shown in (Figure 14) indicate that the contribution of the SAMIs in resisting reflective cracking was more pronounced in specimens tested under a load of 2.4 kN (1.1 MPa) than under 1.35 kN (0.6 MPa), in most cases.

The reason for the better relative performance under a load of 2.4 kN compared to 1.35 kN may be because of the permanent deformation associated with creep at high temperature. Further studies are to be carried out to evaluate the effect of load level at 10°C and 20°C.

Effect of temperature: The effect of temperature on the performance of SAMI 1 and SAMI 2 against reflective cracking was considered by carrying out tests at 10°C, 20°C and 30°C with a 2.4 kN (1.1 MPa) load applied. The results presented in Figure 15 show the number of wheel cycles to failure for the specimens with SAMIs as ratio of those without SAMIs (control). It can be seen from the figure that when an overlay of 40 mm thick was used, the life to failure as ratio of control decreases with increase in temperature, which may be related to change in stiffness of the overlay (Table 2) and SAMI with temperature and the reduction in the stiffness of the overlay-SAMI interface as temperature increases [12]. Also, the figure shows that when an overlay of 60mm was used, the best performance was recorded at 20°C, while the worst performance was observed at 10°C. The reason for this is probably because the overlay becomes brittle due to long exposure to cold temperature (10°C), while it becomes susceptible to permanent deformation at 30°C.

Effect of overlay thickness: The effect of overlay thickness on the performance of the SAMIs was considered by using two different overlay thicknesses of 40 mm and 60 mm for specimens with SAMI 1 and SAMI 2. The results were normalized by dividing the number of cycles to failure of the test specimens by the number of wheel cycles to failure for control specimens of equivalent overall thickness. The results are shown in Figures 16-19.

The figures show that specimens with SAMIs gave better performance against the offset of crack when a 40mm overlay was

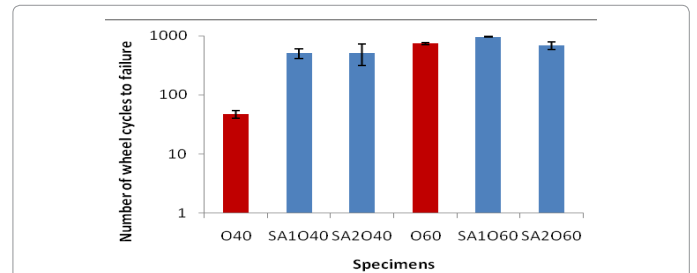


Figure 13: Number of wheel cycles to failure at 30°C with a 1.35kN load applied.

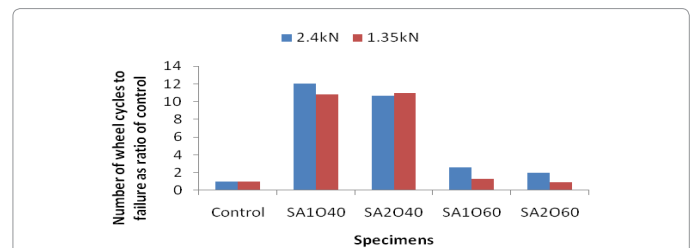


Figure 14: Number of wheel cycles to failure as a ratio of control with 2.4kN and 1.35kN loads applied at 30°C.

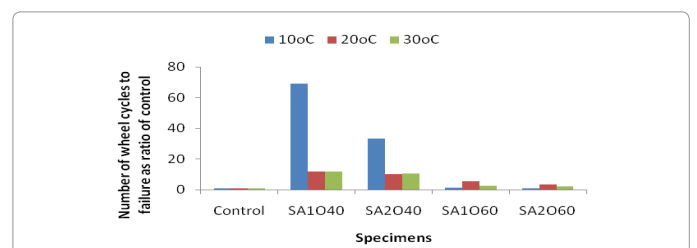


Figure 15: Number of wheel cycles to failure as a ratio of control with a 2.4kN load applied at 10°C, 20°C and 30°C.

used than a 60mm overlay. This indicates that the SAMIs provide better resistance to the offset of crack with a lower overlay thickness. Molenaar et al. [13] found that when SAMIs are used against reflective cracking, a thin overlay would have a longer life than a thick overlay. The reason for the better performance of thinner overlay over a SAMI on a cracked pavement is probably because the SAMI becomes ineffective once crack is initiated at the bottom of the overlay. While it may take greater number of wheel load cycles for the cracks to propagate to the surface when thicker overlay is used, the additional cost of the overlay may outweigh the life gained. Therefore, having thinner overlay over a SAMI provides a better relative benefit than thicker overlay.

Displacement: The initial absolute displacements of the cracked base layer of the specimens are shown in Figure 20. It can be seen that the vertical movement of the specimens increases with increasing temperature. Also the figure shows that lower absolute displacements were measured in the control specimens than in those with SAMIs. This

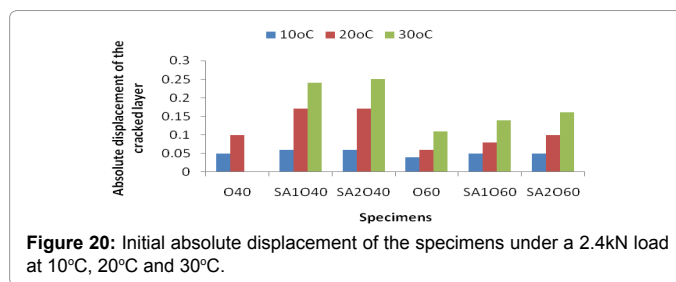


Figure 20: Initial absolute displacement of the specimens under a 2.4kN load at 10°C, 20°C and 30°C.

shows that the increased deflection of the specimen that accompanies the use of the SAMIs does not have a detrimental effect on their performance. The shear strain at the overlay-SAMI interface isolates the overlay from the strain concentration immediately above the base.

Conclusion

This study has shown that the SAMIs evaluated (comprising chopped glass fibre, bitumen emulsion and single-sized aggregate) are able to delay the appearance of cracks in an overlay over a cracked pavement. The degree of improvement varied up to a factor of 69 for thin 40 mm overlay at 10°C. It was discovered that SAMI 1 gave better performance against reflective cracking than SAMI 2, which may be due to the viscosity of the bitumen emulsion used in the SAMIs.

In general, it was found that the SAMIs gave better relative performance when a higher load level was adopted for the trafficking of the specimens. It was also found that the relative benefit of the SAMIs decreased as the overlay thickness increased. This is possibly because the SAMIs become less effective once a crack has been initiated in the overlay. Furthermore, the test results showed that temperature influences the performance of the SAMIs, but in a complex way. The shear strain at the overlay-SAMI interface plays a role in isolating the overlay from strain concentration around the crack region, therefore increasing the life to failure of the overlay. Large scale testing is to be carried out to evaluate the practical/field significance of the study. Also, the use of different types of binder with the glass fibre and modelling of the test are to be considered in future study.

References

- Cleveland GS, Button JW, Lytton RL (2002) Geosynthetic in flexible and rigid pavement overlay systems to reduce reflection cracking. Texas Transport Institute, Texas A&M University System. Report 1777-1.
- Palacios C, Chehab GR, Chaignon F, Thompson M (2008) Evaluation of fiber reinforced bituminous interlayer's for pavement preservation. Proc. 6th International RILEM Conference.
- Von Quintus HL, Mallela J, Weiss W, Shen S (2009) Techniques for mitigation of reflective cracking. Applied Research Associates, Champaign, IL, Interim Report AAPTP 05-04.
- Abe N, Maehara H, Maruyama T, Ooba K (2000) An examination of factor which affects reflective cracking, Proc. 4th International RILEM Conf.
- Smith (1983) Laboratory testing of fabric interlayer's for asphalt concrete paving, Transportation Research Record 916, 6-17.
- Moleenaar AAA (1993) Evaluation of pavement structure with emphasis on reflective cracking, Proc. 2nd International RILEM Conf.
- Al-Qadi IL, Baek J, Buttler WG, (2008) Development of reflective cracking index to determine the effectiveness and service life of strip interlayer systems. Proc. 6th International RILEM Conf.
- Bhosale SS and Mandal JN, (2008) Open graded asphalt concrete for mitigation of reflection cracking on asphalt concrete overlays, Proc. 12th International Conference of International Association for Computer Methods and Advances in Geomechanics (IACMAG).
- BSI (1993) Method for determination of the indirect tensile stiffness modulus of bituminous mixture. British Standard Institution, London, DD 213.

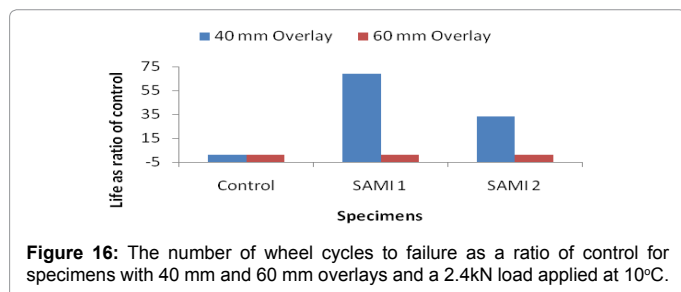


Figure 16: The number of wheel cycles to failure as a ratio of control for specimens with 40 mm and 60 mm overlays and a 2.4kN load applied at 10°C.

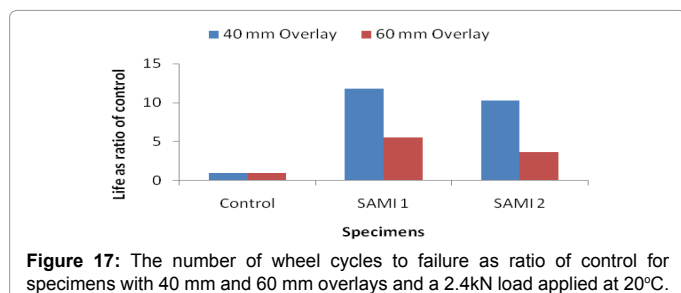


Figure 17: The number of wheel cycles to failure as ratio of control for specimens with 40 mm and 60 mm overlays and a 2.4kN load applied at 20°C.

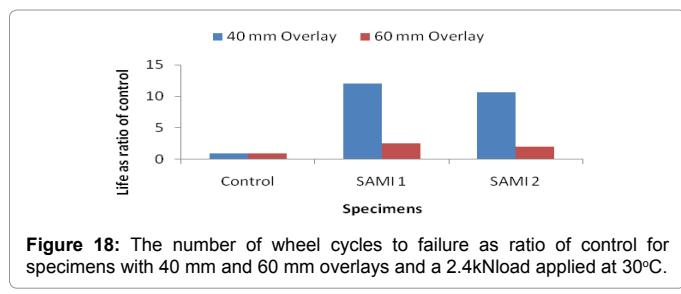


Figure 18: The number of wheel cycles to failure as ratio of control for specimens with 40 mm and 60 mm overlays and a 2.4kN load applied at 30°C.

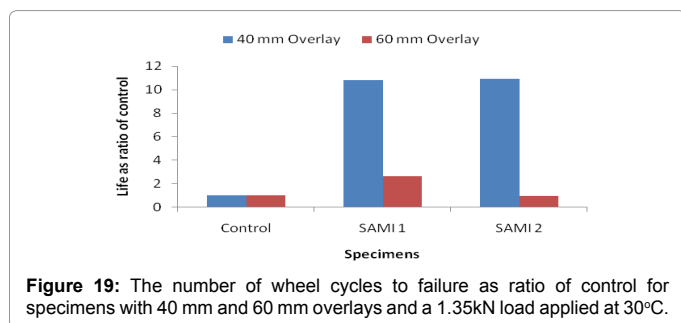


Figure 19: The number of wheel cycles to failure as ratio of control for specimens with 40 mm and 60 mm overlays and a 1.35kN load applied at 30°C.

-
10. BSI (2004) Bituminous mixtures-test method for hot mix asphalt: Laboratory mixing. British Standard Institution, London, BS EN 12697-35.
 11. BSI (2003) Bituminous mixtures-test method for hot mix asphalt: Specimen prepared by roller compactor, British Standard Institution, London, BS EN 12697-33.
 12. Ogundipe OM (2011) Mechanical Behaviour of Stress Absorbing Membrane Interlayers. University of Nottingham, Nottingham.
 13. Molenaar AAA, Heerkens JCP, Verhoeven JMH, (1986). Effects of stress absorbing membrane interlayers, Association of Asphalt Paving Technologists.